Journal of Innovative Optical Health Sciences
Vol. 4, No. 1 (2011) 79−88

DOI: 10.1142/S1793545811001307

WAVELENGTH PROBING OPTICAL COHERENCE TOMOGRAPHY

SHOUDE CHANG and YOUXIN MAO
Imaging Devices Group
Institute for Microstructural Sciences
National Research Council Canada
Ottawa, Ontario, K1A 0R6 Canada

In swept-source optical coherence tomography (SSOCT), the swept-source stimulates system by a series of wavelengths in time sequence; a photo detector then collects all reflected/backscattered light from testing sample as the components of Fourier series. Due to the nature of the SSOCT, the processing in spectral domain can merge multiple swept-sources with different central wavelengths, which greatly increases the resolution of the OCT imaging. In the wavelength probing OCT, a standard broadband SSOCT system is used to extract the internal structure of the sample, and another narrow band light can be used to probe the spectral feature of the sample at the probing wavelength.

Keywords: Optical coherence tomography; swept-source OCT; spectral signal processing.

1. Introduction

Optical coherence tomography (OCT) is a powerful imaging technology for producing high-resolution cross-sectional images of the internal microstructure of materials and/or biological samples. It has been widely used in medical exam and biological testing for more than 10 years.[1−3] OCT relies on the interferometric measurement of coherent backscattering variation to form images of the under-surface structure of test samples like biological tissues or other turbid materials. It takes advantage of the short temporal coherence of a broadband light source to achieve precise optical sectioning in the depth dimension.

Time-domain OCT system is based on a Michelson interferometer. In time-domain OCT (TDOCT) systems, broadband source is used in interferometer. The coherent gate is then created to separate the tomography at a certain layer. A mechanic scanning device is used to select different layers at different depths by moving the reference mirror. The scanning procedure basically determines the processing speed of the whole system.

As the scanning procedure in TDOCT is actually a procedure of convolution, it can be expressed by

$$i_d \propto Es \otimes Er, \tag{1}$$

where Es and Er are the electric fields from sample and reference arms, respectively. $\otimes$ represents convolution, and $\propto$ means "being proportional to". According to the convolution theory, its Fourier transform becomes

$$I_d(\omega) \propto s_s(\omega) \bullet s_r(\omega). \tag{2}$$

where $s_r(\omega) = 1/2s(\omega)$; $s_r(\omega)$ and $s_s(\omega)$ are Fourier transforms of Er and Es, respectively. $s(\omega)$ is the light source spectrum. Considering the interferometer structure, the signal detected by the sensor is given by

$$\begin{aligned} I_d(\omega) &= |s_r(\omega) + s_s(\omega) \bullet s_r(\omega)|^2 \\ &= S(\omega)[1 + s_s(\omega)]^2, \end{aligned} \tag{3}$$

where $S(\omega) = s^2(\omega)$. Equation (3) is the foundation of Fourier domain OCT (FDOCT) or spectral domain OCT (SDOCT).[4,5]

SDOCT extracts the spectral signal by means of a grating spectrometer and a linear detector array. The reconstruction of the internal tomography is performed by an inverse Fourier transform of $I_d(\omega)$. Instead of using a simultaneous broadband light source and a spectrometer, swept-source OCT (SSOCT) uses a swept laser as the light source. SDOCT gets all the broadband $I_d(\omega)s$ in one shot but collects the signal in series from the linear detector array. However, SSOCT collects the spectral signal in series by changing the wavelength of the light source. Both need an additional inverse Fourier transform, implemented by either hardware or software.

FDOCT and SDOCT have several advantages over TDOCT. Because of no mechanic scanning, the FDOCT system is significantly faster, 50 to 100 times, than TDOCT.[6] In addition, both FDOCT and SSOCT have better sensitivity and signal-to-noise ratio.[7,8]

2. SSOCT Spectral Signal

In SSOCT, the broadband light source plays an important role. The linewidth and output power determine the imaging range of an SSOCT system. The bandwidth of the light source places the main barrier for the imaging resolution. At current stage, most commercial swept-sources have a bandwidth of about 100 nm corresponding to an axial resolution around 14 μm in air.

In SSOCT, the swept-source stimulates the system by a series of wavelengths in time sequence; a photodetector then collects all the responses as Fourier series components of testing sample. Because the detector is only sensitive to optical power, it loses the phase information in the reflected/backscattered signal. At any moment, the signal detected by sensor can be written as

$$I(k) = |E(k)H(k)|^2, \quad k = 1, 2, 3, 4, \ldots, N, \quad (4)$$

where $E(k)$ is the kth wavelength sent from source, $H(k)$ is the response function for all scatters within depth range, and $I(k)$ is the signal generated by the sensor. Assuming $S(k) = |E(k)|^2$, power spectrum of the light source, the output of an interferometer-based OCT system can be expressed by

$$I(k) = S(k)[H(k) + 1]^2. \quad (5)$$

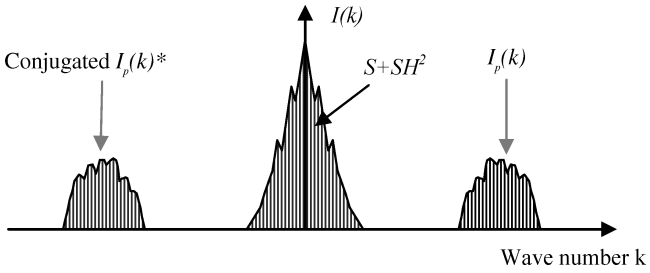

Fig. 1. SSOCT signal.

Normally, $S(k)$ is a Gaussian function; to completely eliminate its effect in the reconstruction, a deconvolution may be required in post-processing. In this paper, either in simulation or experiments, we take $S(k)$ as an even-distributed function, i.e., a constant.

Extending (5), $I(k) = S(k)H^2(k) + 2S(k)H(k) + S(k)$. Taking $S(k)$ as a constant and $H^2(k)$ as low-frequency component that can be ignored, the processed $I(k)$ becomes

$$I_p(k) = CH(k), \quad (6)$$

where C is a constant. Figure 1 shows $I(k)$ and $I_p(k)$. The reconstruction of the sample in spatial domain (depth z) can be performed by an inverse Fourier transform:

$$h(z) = IFT[I_p(k)]. \quad (7)$$

Equation (7) works only when the light source is a simultaneous broadband source, which provides all the wavelengths at the same time. This is the base for spectral domain OCT. However, in SSOCT, the sweeping wavelength k is a function of time. In this case, at any moment, Eqs. (6) and (7) are the results from one wavelength. When all the $I_p(k)$s with different wavelengths form a sequence,

$$I_s(k) = \sum\nolimits_n I_p(k)\delta(k-n), \quad n = 1, 2, \ldots, N. \quad (8)$$

The internal structure of the sample can then be extracted by

$$h(z) = IFT[I_s(k)] = IFT\Big[\sum\nolimits_n CH(k)\delta(k-n)\Big], \quad (9)$$

where $\delta(k-n)$ is used to separate each Fourier series component at a discrete k number, as illustrated in Fig. 2.

In Eq. (9), each wavelength response $H(k)\delta(k-n)$ carries two types of information: (a) structure

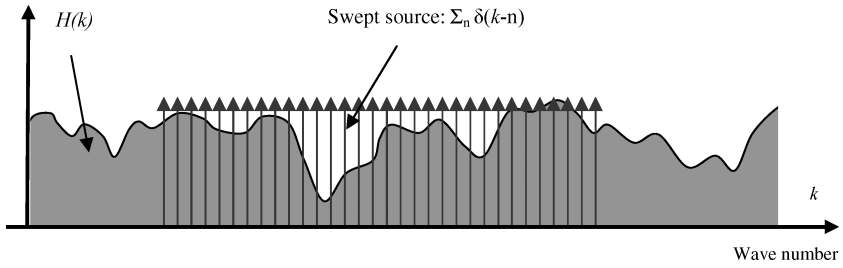

Fig. 2. Swept-source discrete spectrum.

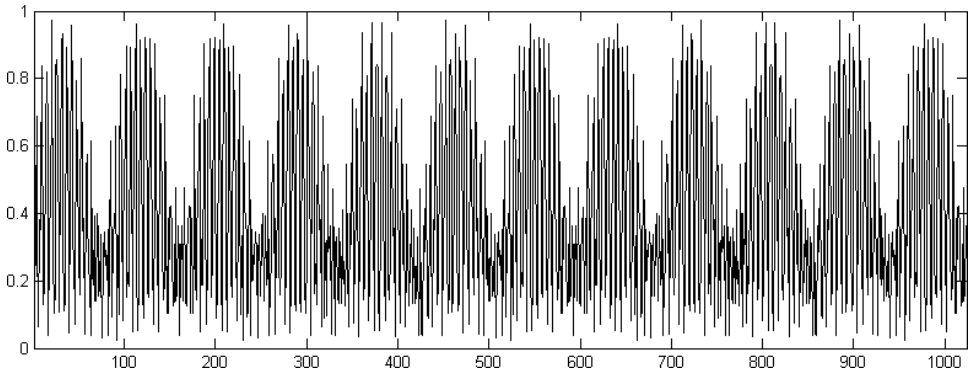

Fig. 3. SSOCT spectral signal simulated from a three-layer glass slide.

information of all internal layers corresponding to depth z; (b) spectral information corresponding to wavelength number k. The more wavelengths (bigger N), the finer resolution or richer structure can be reconstructed. N stimulating wavelengths determine the shape of the structure; however, there is no proof that those N wavelengths must be distributed uniformly. Different positions of stimulating wavelengths may provide different spectral information, relying on the $H(k)$ of the sample. For example, W wavelengths may reconstruct N layers. If N layers have different absorption rates corresponding to different wavelengths, the change of wavelength can affect the "color" of layers reconstructed. In other words, the number of wavelengths defines the number of reconstructed layers; the positions of the wavelengths related to $H(k)$ determine the colors of layers.

Figure 3 shows the SSOCT spectral signal simulated from a three-layer glass slide. The first two slides have a thickness of 1 mm. The last one has a thickness of 2 mm. All slides have reflective index of 1.5. The air gap is 0.1 mm. Totally, 1,024 wavelengths with equal intensity are used as the light source. In the SSOCT spectrum, 1,024 wavelength points are presented. Figure 4 shows the

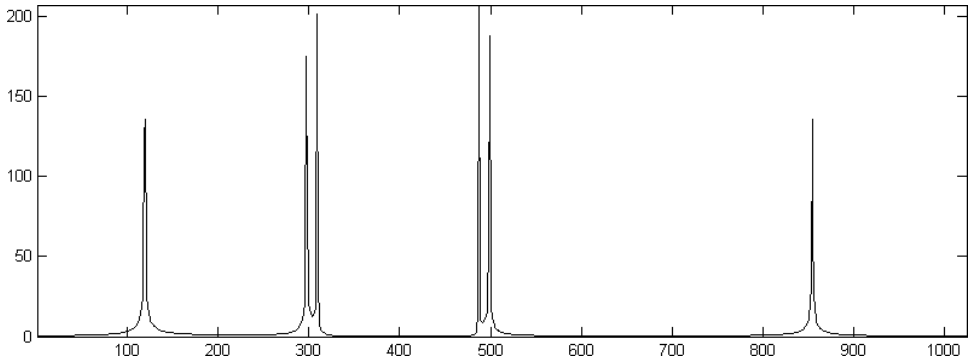

Fig. 4. The reconstruction of the three-layer glass slide shown in Fig. 3.

reconstructed OCT image. Six impulses indicate the six interfaces between the slides and air.

3. Wavelengths Splitting/Integration

The spectrum of SSOCT has the following features:

(1) The input is a series of laser impulses. Only one wavelength exists at any moment.
(2) Spectrum is a set of N discrete signals $\sum_N H(k)\delta(t-k)$.
(3) Spectral variable is wavenumber $k = 2\pi/\lambda$, where λ is wavelength.
(4) As the sensor cannot detect phase information, directly reconstructed OCT image has a conjugate part (mirrored image).
(5) No DC and low-frequency components.

Because of no DC and low-frequency components, as shown by $S + SH^2$ in Fig. 1, SSOCT signal is different to the pattern directly Fourier-transformed from the spatial structure. Figure 5 shows the result of direct Fourier transform of the structure shown in Fig. 4, in which low- and high-frequency components behave differently from that in Fig. 3. Lower frequency normally contributes to large area structures, and higher frequency is responsible for the small details in spatial structure. Unlike the spectrum in Fig. 1, the DC and low-frequency components as well as high-frequency components are closely fused together, so that there is almost no way to separate them apart.

In SSOCT signal, each wavelength line makes individual contribution to the reconstruction. After inverse Fourier transform, a single wavelength, i.e., a δ function impulse will become a flat curve, which contains no structure of the sample. When multiple wavelengths are used, the meaningful structure appears. The more the spectral lines, the more details will come out. The resolution of the reconstructed image is given by the total number of spectral lines, with less relation to the location of those lines, assuming that the spectrum of sample $H(k)$ is constant.

A δ function impulse contains no structure information. However, for a conjugated pair of δ function, its Fourier transform becomes a sinusoidal wave, rather than a flat curve. Such a $\sin(z)$ function wave can change the shape of any curve when it has been added to, which means that a single complex wavelength also carries the structural information.

Figure 6 provides a set of reconstructed images of Fig. 3 after different processing. Figures 6(a) and 6(b) show the reconstructed images after 100 point low-pass and high-pass filtering, respectively. Figure 6(c) shows the image after bandpass filtering: only the middle 100 points in Fig. 3 are taken into the inverse Fourier transform. Figure 6(d) shows the result from a bandstop filtering. Those images show almost the same reconstructed structure. Because only 10% wavelength components are taken into the reconstruction, those images are much coarser than that shown in Fig. 4. Those results also show that no matter where the locations of spectral lines are, they contain similar shape information.

Because SSOCT has a swept wavelength source, there is a time difference between wavelengths passed to the system. In addition, as the sensor is not able to detect phase information, there is no coherence among different wavelengths, especially when time becomes longer. Each wavelength independently makes its contribution to the reconstruction as a Fourier series component. This feature gives SSOCT a possibility to increase the bandwidth by combining multiple swept-sources,

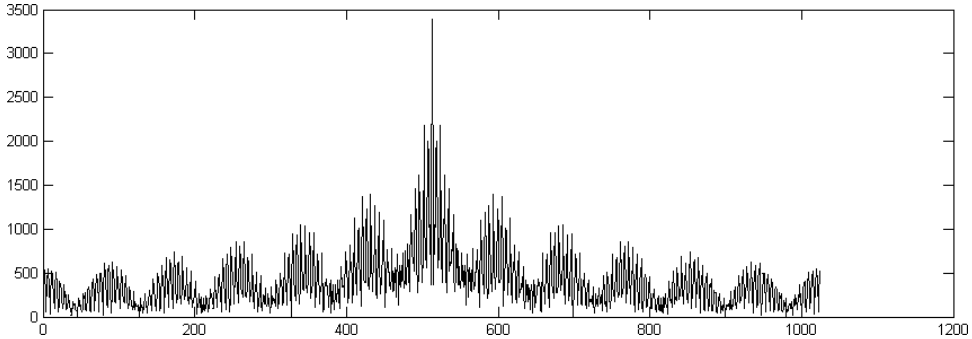

Fig. 5. Direct Fourier transform of Fig. 4.

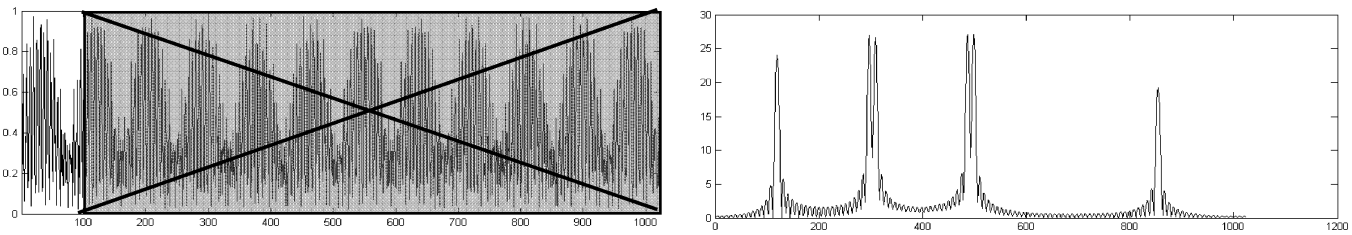

(a) Left: SSOCT signal after high-pass filter. Right: Reconstructed image of left.

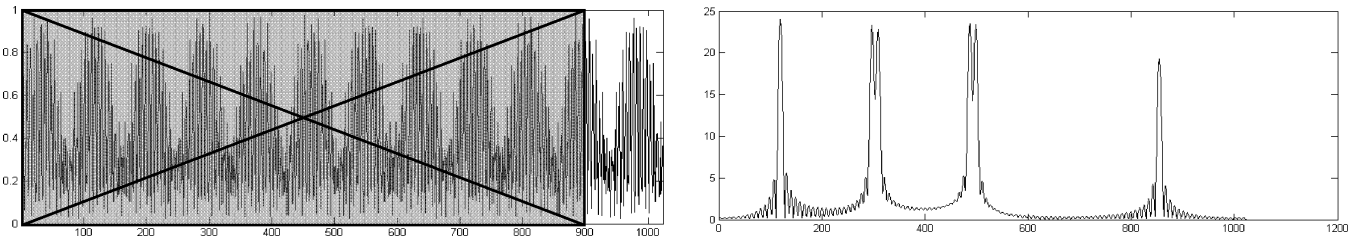

(b) Left: SSOCT signal after low-pass filter. Right: Reconstructed image of left.

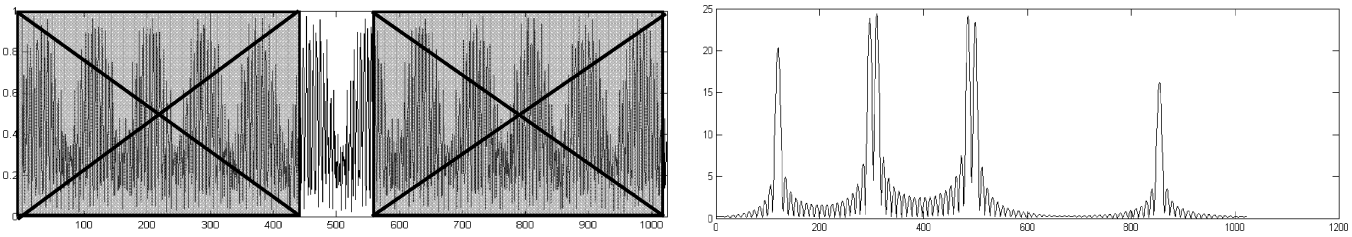

(c) Left: SSOCT signal after bandpass filter. Right: Reconstructed image of left.

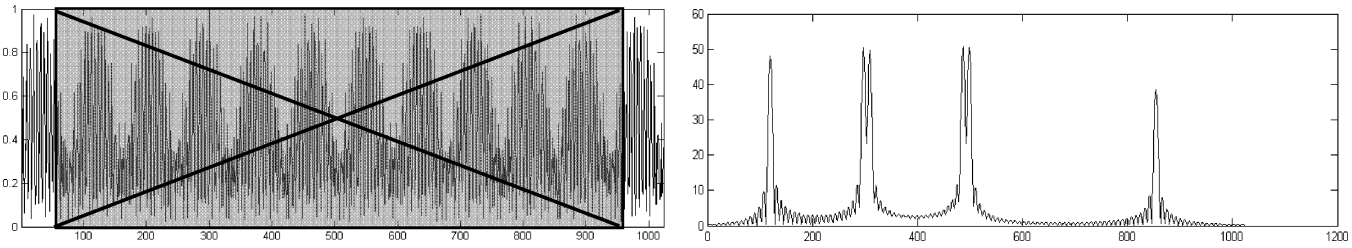

(d) Left: SSOCT signal after bandstop filter. Right: Reconstructed image of left.

Fig. 6. SSOCT signal filtering and reconstruction.

which have different central wavelengths. When two swept-sources $S_1(k)$ and $S_2(k)$ (see Fig. 7) are used with different parameters: central wavelength $(k01, k02)$; impulse interval $(\Delta k1, \Delta k2)$; and impulse intensity $(A1,\ A2)$, the combined swept-source becomes $S(k) = S_1(k) + S_2(k)$. And the combined SSOCT spectrum is given by

$$I(k_c) = a_1 S_1(k_c) H(k_c) + a_2 S_2(k_c) H(k_c), \qquad (10)$$

where k_c is the new k scale in the combined discrete spectrum, and the new interval Δk_c is the maximal common divisor of Δk_1, Δk_2. To have all the wavelengths in different sources make the same contribution to reconstruction, coefficients a_1 and a_2 are introduced so that $a_1 A_1 = a_2 A_2$.

Figure 8 shows computer simulations of two sources' combination. Two SSOCT spectral signals $S_1(k)H(k)$ and $S_2(k)H(k)$, each having 80 wavelength points with 960 wavenumber separation between them, are combined together. The reconstructed image shows higher spatial resolution than those separately reconstructed from two sources.

Most of the OCT applications have been developed for biomedical imaging and diagnosis.[9] Besides exploring the internal structures, OCT can also provide spectroscopic information of the testing

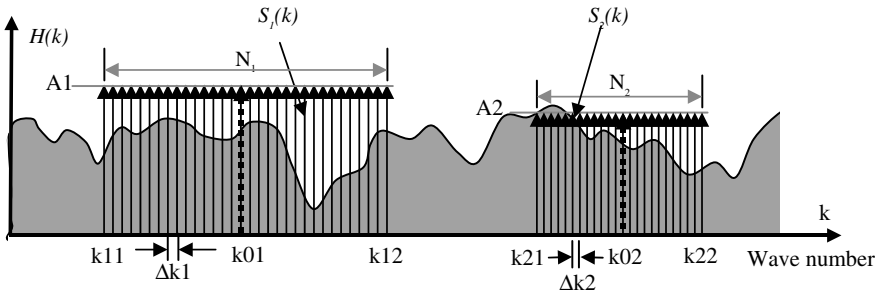

Fig. 7. Spectrum of two light sources.

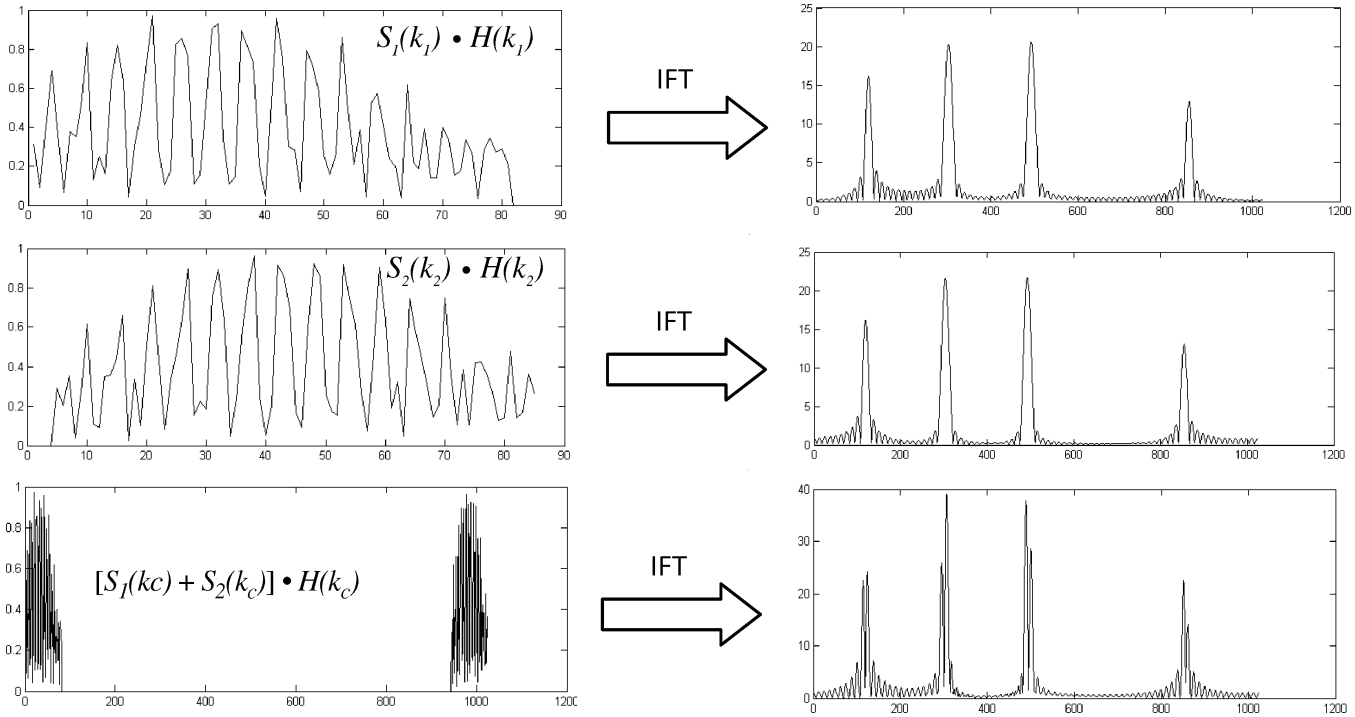

Fig. 8. Integration of two sources.

sample.[10,11] The broader the bandwidth of the light source, the more spectral features can be extracted out. Depending on specific medical application, the meaningful spectral feature may exist at different wavelengths. For example, the absorption spectra of a normally perfused skin flap and one that has abnormal blood supply show an obvious difference at 650 nm.[12] Therefore, the central wavelength of the light source is critical for spectral feature extraction. In Ref. 13, a method has been proposed to find the subspectral feature inside a structure by using two different filtering windows. However, this method is limited to the case where the featuring subspectrum must be located inside the band of the source. It will be ideal to have a central wavelength-tunable swept-source to suit different kinds of applications. Being originally developed for the fiber communication, the commercial swept-sources are inherently limited only around 1,300 nm and 1,500 nm. Even if a central wavelength-tunable swept-source could be fabricated, the price of the device may be very expensive.

4. OCT with Probing Wavelength

Equation (10) enables the integration of a commercially available broadband swept-laser source and a narrow band source. The broadband source is used to build internal structure, and the narrow band source, namely, probing wavelength (PW), is

used to explore spectral feature. PW light should have the central wavelength close to the "featuring" wavelength of the testing sample. When S_1 is a broadband source with a bandwidth of N_1, $S_1(k) = 1; k \in (k11 : k12)$. And S_2 is a narrow band source with a bandwidth N_2, $N_2 < N_1$, $S_2(k) = 1; k \in (k21 : k22)$. The output of an SSOCT system is

$$I_s(k) = \sum H(k)S_1(k) + \sum H(k)S_2(k). \qquad (11)$$

As a function of spectral feature of sample, $H(k)$ may change at different wavelengths. Assuming $H(k) = 0; k \in (k12 : k21)$, even if the light source has a large enough broadband, $I_s(k)$ still has a discontinuous area: $I_s(k) = 0$, $k \in (k12 : k21)$. Hence,

$$I_s(k) = \sum_{k11}^{k22} H(k)S(k)$$

$$= \sum_{k11}^{k12} H(k)S(k) + \sum_{k21}^{k22} H(k)S(k). \qquad (12)$$

The two-source combination with a blank area can be considered that a continuous broadband source $S(k)$, $k \in (k11 : k22)$ with a sample whose spectrum has 0 values in the blank area $k \in (k12 : k21)$. The second item in the right-hand side of Eq. (12) can be a broadband source or a narrowband source — the probing wavelength WP. Because the probing wavelength is a narrowband source in the combined spectrum, it has to be boosted by a weighting factor p, in order to enhance the contribution of this probing wavelength in the reconstruction. Hence, Eq. (12) becomes

$$I_s(k) = \sum_{k11}^{k22} H(k)S(k)$$

$$= \sum_{k11}^{k12} H(k)S(k) + p\sum_{k21}^{k22} H(k)S(k). \qquad (13)$$

Assuming a wavelength $k_f \in (k21 : k22)$ is the featuring wavelength of a sample, at this wavelength,

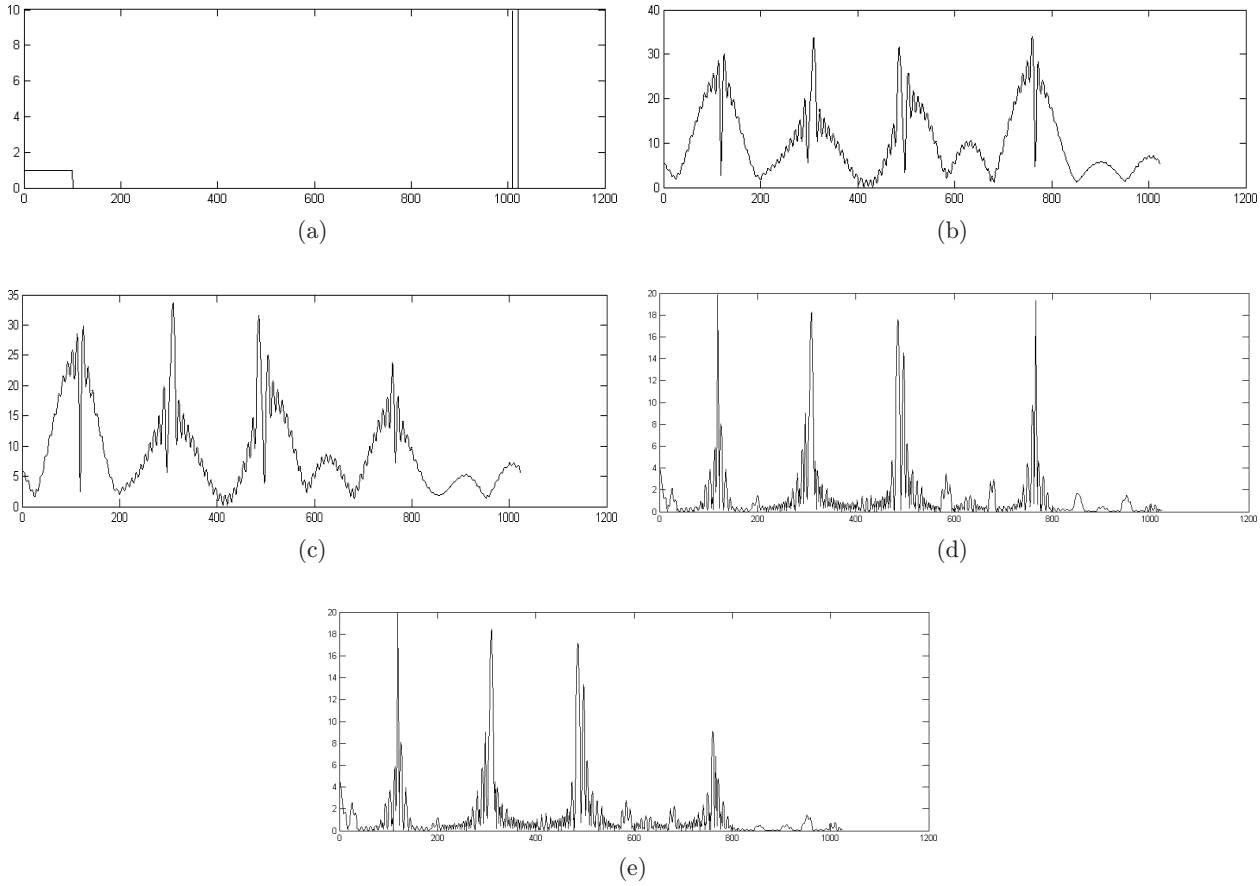

Fig. 9. Reconstructed results with wavelength probing OCT described in Test 1. (a) Source. Broadband: 100 spectral points. Narrowband: 10 spectral points. (b), (c) Reconstructed OCT images for "abnormal" and "normal" samples. (d) High-pass filtering of (b). (e) High-pass filtering of (c).

the normal spectrum of the sample is $H_1(k)$, and abnormal is $H_2(k)$. The corresponding SSOCT signals are

$$I_{s1}(k) = \sum_{k11}^{k12} H(k)S(k) + p\sum_{k21}^{k22} H_1(k)S(k), \quad (14)$$

$$I_{s2}(k) = \sum_{k11}^{k12} H(k)S(k) + p\sum_{k21}^{k22} H_2(k)S(k). \quad (15)$$

Since $H_1(k) \neq H_2(k)$, $I_{s1}(k) \neq I_{s2}(k)$. The dif- ference $I_{s1}(k) - I_{s2}(k)$ between those reconstructed tomograms reflects the spectral changes of the testing sample.

5. Computer Simulation

To verify the wavelength probing SSOCT described above, computer simulations were carried out. A 100 nm bandwidth source centered at 1,300 nm is used as the broadband source, which is arranged to cover 1:100 spectral lines. The narrowband probing wavelength is located at the 1,015:1,024 spectral lines. The sample is the same as that used in Fig. 3. For the broadband source, all glass slides have the same spectral response $H(k)$. However, for the probing wavelength, the last glass slide has different spectral responses corresponding to "normal" and "abnormal" statuses. For the "normal", the transmission ratio is set $T1 = 0.8$, but for the "abnormal", this ratio is set $T2 = 0.6$. The transmission ratio is defined as the ratio of $\text{Power}_{\text{out}}/\text{Power}_{\text{in}}$. If the ratio is low, it means more energy is absorbed inside the sample. The weighting factor for probing wavelength is set as $p = 10$.

In Test 1, the broadband source has a bandwidth of 100 points while narrowband has 10 points, which form a combined light source as shown in Fig. 9(a). The reconstructed image by IFFT$[I_{s1}(k)]$ (with $T1$) representing "normal" is shown in Fig. 9(b), while the reconstructed "abnormal" image by IFFT$[I_{s2}(k)]$ (with $T2$) is shown in Fig. 9(c). Because of the

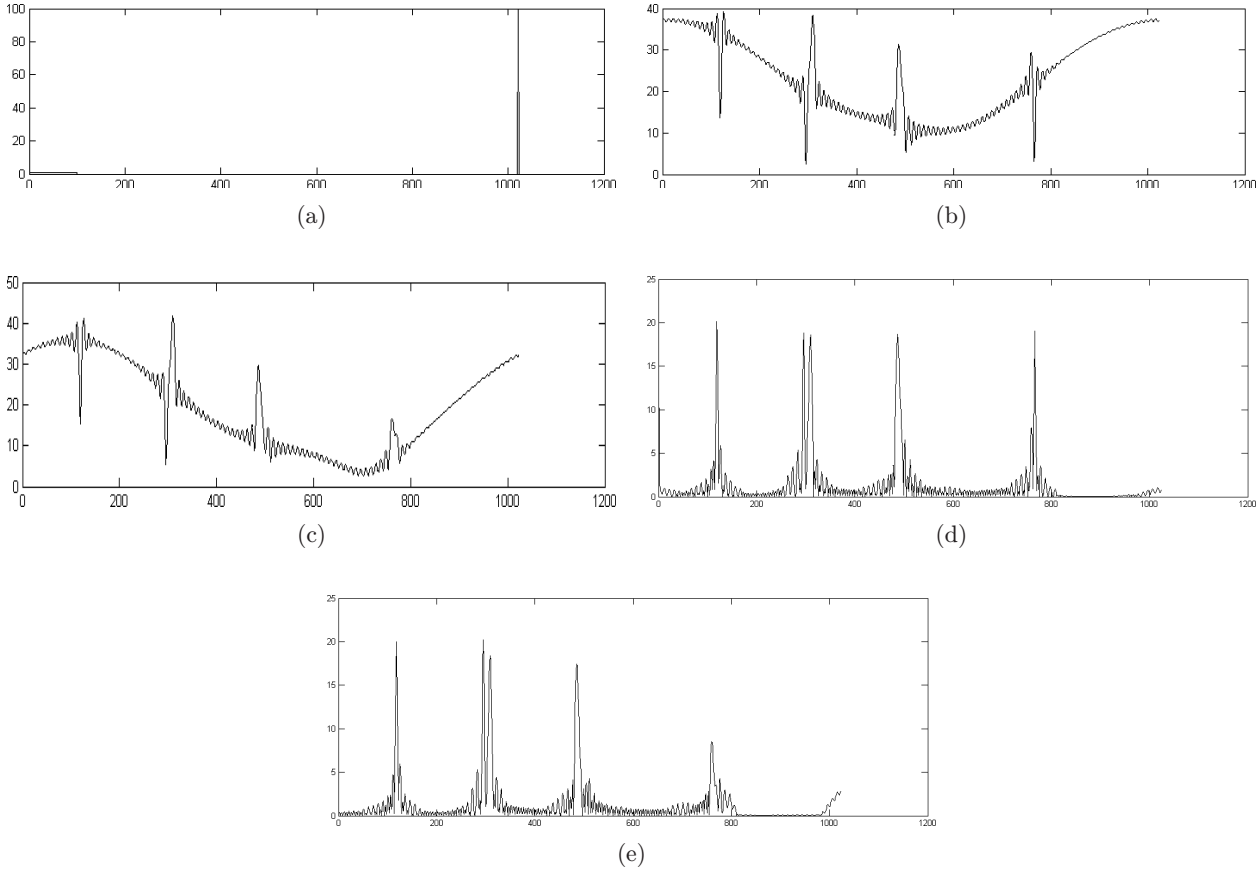

Fig. 10. Reconstructed results with wavelength probing OCT described in Test 2. (a) Source. Broadband: 100 spectral points. Narrowband: 2 spectral points. (b), (c) Reconstructed OCT images for "abnormal" and "normal" samples. (d) High-pass filtering of (b). (e) High-pass filtering of (c).

side-effect of weighting factor p in Eqs. (14) and (15), both the reconstructed images have a floating main curve being introduced. In Test 1, as 10 spectral lines are used and emphasized by p, there are five periodic floatings added in the glass slide structure. In Test 2, because only two spectral lines are used and emphasized, one period wave has been added on the glass slide structure. All those low-frequency floating curves can easily be removed by a high-pass spatial filter. Figures 9(d) and 9(e) show the results after high-pass filtering. It is evident that the last peaks in (d) and (e) are different. Those results show that the spectral difference basically happens at the position where the last glass slide is located. In Test 2 simulation, all the conditions are given the same as those in Test 1. But the probing wavelength has a very narrower band: only two spectral lines (see Fig. 10 (a)). The reconstructed "normal" and "abnormal" OCT images are shown in Figs. 10(b) and 10(c), respectively. Similarly, a high-pass filtering is performed for both "floating curves". Figures 10(d) and 10(e) show the final results. Obviously, the biggest difference is still located at the third layer position. Note that all the layers still stand there, but the relative intensity of each peak has been changed slightly, because of the p value introduced and high-pass filtering.

6. Summary and Discussion

SSOCT is based on a series of wavelength impulse responses as Fourier series decomposition. Each impulse response contains two types of information for reconstruction: internal structures and spectral feature of the sample. As SSOCT signal contains no DC and low-frequency components, each spectral line makes equal contribution to the reconstruction. The more spectral lines in SSOCT signal, the more details will be created in the reconstructed image. The linewidth of the spectral line defines the imaging depth, and the total number of spectral lines contained in SSOCT spectrum gives the depth resolution. Because only one wavelength exists at any moment and almost no coherence between the sweeping wavelengths, it is possible to integrate the OCT signals obtained from multiple swept-sources to extend the effective bandwidth and eventually enhance the axial resolution of the reconstructed OCT image.

Based on spectrum integration, a standard SSOCT combined with a narrowband light source can not only build the internal structure of the testing sample, but also provide the spectral information corresponding to the probing wavelength. Computer simulations show that this idea works. By means of spectral domain processing, multiple broadband swept-sources responses could be combined together to further extend the bandwidth, and therefore greatly increase the axis resolution and extract more spectroscopic information.

References

1. D. Huang, E. A. Swanson, C. P. Lin, J. S. Schman, W. G. Stinson, W. Chang, M. R. Hee, T. Flotte, K. Gregory, C. A. Pullafito, J. G. Fujimoto, "Optical coherence tomography," *Science* **254**, 1178−1181 (1991).
2. W. Drexler, J. G. Fujimoto, *Optical Coherence Tomography, Technology and Applications*, Springer-Verlag, Berlin, Heidelberg (2008).
3. G. Smolka, *Optical Coherence Tomography: Technology, Markets, and Applications 2008−2012*, BioOptics World. Penn Well Corporation (2008).
4. S. R. Chinn, E. A. Swanson, J. G. Fujimoto, "Optical coherence tomography using a frequency-tunable optical source," *Opt. Lett.* **22**, 340−342 (1997).
5. M. A. Choma *et al.*, "Sensitivity advantage of swept source and Fourier domain optical coherence tomography," *Opt. Exp.* **11**, 2183−2189, ISSN:1094-4087 (2003).
6. S. H. Yun, G. J. Tearney, J. F. de Boer, N. Iftimia, B. E. Bouma, "High-speed optical frequency-domain imaging," *Opt. Exp.* **11**, 2953−2963 (2003).
7. J. F. de Boer *et al.*, "Improved signal-to-noise ratio in spectral-domain compared with time-domain optical coherence tomography," *Opt. Lett.* **28**, 2067−2069, ISSN:0146-9592 (2003).
8. R. Leitgeb, C. K. Hitzenberger, A. F. Fercher. "Performance of Fourier domain vs. time domain optical coherence tomography," *Opt. Exp.* **11**, 889−894, ISSN:1094-4087 (2003).
9. W. Drexler, J. G. Fujimoto, *Optical Coherence Tomography, Technology and Applications*, Springer-Verlag, Berlin Heidelberg (2008).
10. U. Morgner, W. Drexler, F. X. Kartner, X. D. Li, C. Pitris, E. P. Ippen, J. G. Fujimoto, "Spectroscopic optical coherence tomography," *Opt. Lett.* **25**, 111−113 (2000).
11. R. Leitgeb, M. Wojtkowski, A. Kowalczyk, C. K. Hitzenberger, M. Sticker, A. F. Fercher, "Spectral measurement of absorption by spectroscopic frequency-domain optical coherence tomography," *Opt. Lett.* **25**(11), 820−822 (2000).

12. D. J. Faber, M. C. G. Aalders, E. G. Mik, B. A. Hooper, M. J. C. van Gemert, T. G. van Leeuwen, "Oxygen saturation-dependent absorption and scattering of blood," *Phys. Rev. Lett.* **93**, 028102 (2004).

13. F. Robles, R. N. Graf, A. Wax, "Dual window method for processing spectroscopic optical coherence tomography signals with simultaneously high spectral and temporal resolution," *Opt. Exp.* **17**(8), 6799−6812 (2009).